

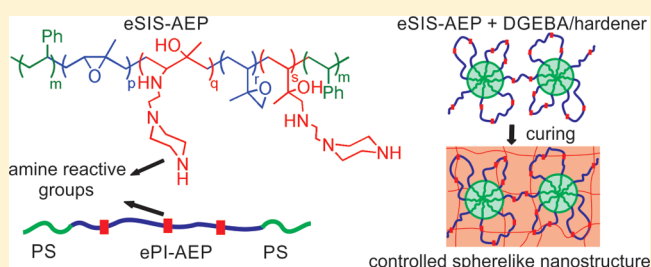
# Controlling Nanodomain Morphology of Epoxy Thermosets Modified with Reactive Amine-Containing Epoxidized Poly(styrene-*b*-isoprene-*b*-styrene) Block Copolymer

Hernan Garate,<sup>†,‡</sup> Silvia Goyanes,<sup>\*,‡</sup> and Norma B. D'Accorso<sup>\*,†</sup>

<sup>†</sup>CIHIDECAR-CONICET; Departamento de Química Orgánica, FCEyN – UBA, and <sup>‡</sup>IFIBA – CONICET; LP&MC, Departamento de Física, FCEyN – UBA, Ciudad Universitaria, 1428, Ciudad Autónoma de Buenos Aires, Argentina

## Supporting Information

**ABSTRACT:** Controlling nanodomain morphology of nanostructured epoxy thermosets is critical to modulate the mechanical properties of the cross-linked matrix. In this contribution, we demonstrate that this can be achieved by using a suitable block copolymer containing an epoxy soluble block with the ability to react toward the epoxy system during curing. For this purpose we designed an epoxidized poly(styrene-*b*-isoprene-*b*-styrene) block copolymer incorporating amine-reactive functionalities (eSIS-AEP) in the epoxidized block as modifier for an epoxy system, which allowed the formation of nanostructured thermosets with controlled spherulike nanodomain morphology. The eSIS-AEP was obtained in two steps from poly(styrene-*b*-isoprene-*b*-styrene) (SIS) block copolymer by controlled epoxidation of the olefinic block followed by partial oxirane ring-opening reaction using 1-(2-aminoethyl)piperazine as nucleophile. Before the curing reaction it was observed that poly(styrene) blocks self-assembled to form ordered spherulike nanostructures in blends of eSIS-AEP with epoxy precursors. Since the amine-reactive moiety was incorporated to the block copolymer so that it could react toward diglycidyl ether of bisphenol A (DGEBA) at a similar temperature than the DGEBA/hardener reaction, the epoxy miscible block of eSIS-AEP (ePI-AEP) was able to react with DGEBA during curing. Once the cross-linked network was formed, the initially obtained spherulike nanodomains were preserved, indicating that no reaction-induced microphase separation of ePI-AEP subchains occurred. A completely different scenario was ascertained for epoxidized SIS block copolymer, which conducted to nonspherical nanodomains due to the uncontrolled epoxidized poly(isoprene) demixing process during the curing reaction. These results demonstrate the importance of the epoxy soluble block being reactive toward the epoxy precursors to control the morphology of the obtained nanostructure.



## INTRODUCTION

Inducing nanometer-scale architectures inside epoxy thermosets by the incorporation of suitable block copolymers (BCPs) has emerged as a convenient strategy to further optimize epoxy thermoset material properties.<sup>1–4</sup> It is well-documented that depending on the solubility of the different blocks with the epoxy precursors, the obtained morphologies can be formed by self-assembly<sup>5–10</sup> or by reaction-induced microphase separation (RIMPS).<sup>11–15</sup> The self-assembly approach generally involves mixing block copolymers that contain epoxy soluble and epoxy insoluble segments with the epoxy precursors. The developed nanodomains can be locked during the curing reaction. On the other hand, the RIMPS process involves block copolymers that contain epoxy soluble blocks. As the polymerization reaction proceeds, one block undergoes phase separation due to immiscibility with the thermosetting matrix, leading to the nanostructured thermoset. By exploiting these strategies, a great variety of different morphologies can be induced inside the thermosetting matrix ranging from spherulike to lamellar nanostructures.<sup>16–19</sup>

In the past few years, many researchers have been studying the fundamentals of structure–property relationships in nanostructured thermosets modified with BCPs.<sup>20–26</sup> It has been realized that substantial toughness improvements at low block copolymer loadings can be achieved by incorporating vesicles, cylinders, spheres, or wormlike vesicles, while the effect on other important properties, such as the Young's modulus, strongly depends on the nanodomain morphology.<sup>25,27</sup> Therefore, understanding the parameters that determine the operating nanostructure formation mechanisms arises as a major issue that once it has been overcome would give access to controlled nanodomain morphologies and therefore nanostructured thermosetting materials with finely tuned mechanical properties.

Recent works by Bates and co-workers<sup>4</sup> showed that the toughening mechanisms in the epoxy thermosets modified with block copolymers are strongly influenced by the epoxy/block

Received: July 21, 2014

Revised: October 6, 2014

Published: October 21, 2014

copolymer interphase, which depends on the nanodomain morphology. For nonreactive block copolymers the epoxy/block copolymer interphase becomes thicker by modifying epoxy systems with weak amphiphilic BCPs, while strong amphiphilic BCPs conduct to narrower interphases, as described by Sun et al.<sup>28</sup>

A very different scenario might be the case for reactive block copolymers as modifiers, which contain functional groups capable of reacting toward the epoxy precursors. In this field, Bates and colleagues<sup>29</sup> and Guo and co-workers<sup>17</sup> studied the modification of epoxy thermosets with block copolymers bearing poly(methyl acrylate-*stat*-glycidyl methacrylate) and poly(glycidyl methacrylate) as reactive blocks, respectively. Similarly, Leibler and co-workers,<sup>2,30</sup> reported methacrylate and statistical copolymers of methyl methacrylate with acrylic acid as reactive blocks. In such systems, the epoxy-soluble block can be trapped inside the thermosetting matrix as the curing reaction proceeds, while the epoxy-insoluble block becomes microphase separated. However, a thorough understanding of reactive block copolymers as thermosetting modifiers is relegated to only a few studies, and the question of how the BCP reactivity affects the nanodomain morphology remains still unexplored.

More recently, we have demonstrated that epoxidized SIS (eSIS) block copolymer induces nanostructures inside epoxy thermosets by a mechanism comprising two steps: a first self-assembly of poly(styrene) (PS) blocks that leads to spherulike structures, followed by a partial RIMPS process of epoxidized poly(isoprene) (ePI) blocks. The latter produces a distortion in the interphase of the PS nanospheres shifting to disordered wormlike nanodomains.<sup>31</sup> This morphological shift was proposed to be due to the lower reactivity of trisubstituted oxirane ring of ePI repeating unit respect to the terminal oxirane rings of DGEBA monomer toward the curing agent.

Herein, we focused our attention on controlling the spherical nanodomain morphology developed by the self-assembly of epoxidized SIS block copolymer inside an epoxy matrix. Such block copolymer can be obtained by epoxidation of commercial SIS block copolymer<sup>32</sup>—the most successful BCP product in the worldwide marketplace. Based on our previous results, it was anticipated that if partial RIMPS of ePI block was avoided, the initial spherulike nanostructures obtained by PS blocks self-assembly would be locked through the curing process, and therefore the morphology would be preserved. To evaluate this hypothesis, and following a similar strategy than that proposed by Bonnaud et al.<sup>33</sup> where amino groups were grafted to the backbone of a poly(ether imide), in this work we attempted to increase the reactivity of ePI subchains toward the epoxy precursors by partial oxirane ring-opening reaction with 1-(2-aminoethyl)piperazine (AEP) as the nucleophile. By this strategy, amino groups capable of reacting with DGEBA at a similar temperature as DGEBA/hardener reaction were introduced to the epoxy-soluble block of eSIS to give a novel reactive block copolymer (eSIS-AEP). To the best of our knowledge, this is the first report focusing on incorporating amino reactive moieties to the epoxy-soluble block of the BCP to provide reactivity toward the epoxy monomer. By this modification the question of how the BCP reactivity affects the interphase nanodomain structure and therefore the final nanodomain morphology could be addressed by a comparative analysis of the reactive eSIS-AEP against the unmodified eSIS, which is less reactive toward the epoxy resin.<sup>31</sup>

Therefore, the purpose of this work is twofold: to synthesize a new block copolymer derived from epoxidized SIS BCP, containing amino groups capable of reacting with DGEBA monomer at a similar temperature than DGEBA/hardener reaction, and to study its application as modifier to obtain nanostructured epoxy thermosets with controlled nanodomain morphology. Such studies would contribute to a better insight into the molecular mechanism responsible for the nanodomain formation and evolution in nanostructured thermosetting materials.

## EXPERIMENTAL SECTION

**Materials.** A commercial cylinder forming poly(styrene-*b*-isoprene-*b*-styrene) (SIS) block copolymer Kraton SIS-D1165 was epoxidized in 100% (eSIS) using a previously reported strategy.<sup>32</sup> Triethylamine, 1-(2-aminoethyl)piperazine, and anhydrous THF were purchased from Sigma-Adrich and used as received without further purification. The epoxy monomer, diglycidyl ether of bisphenol A (DGEBA), Epikote 828, was purchased from Hexion. It has an epoxy equivalent of around 184–190. The hardener was a mixture of amines under the commercial name of Ancamine 2500 (1-(2-aminoethyl)-piperazine:1,3-bis(aminomethyl)benzene; 1:2 mol/mol), supplied by Air Products. The chemical formulas of all the epoxy components used for this study are given in Figure 1.

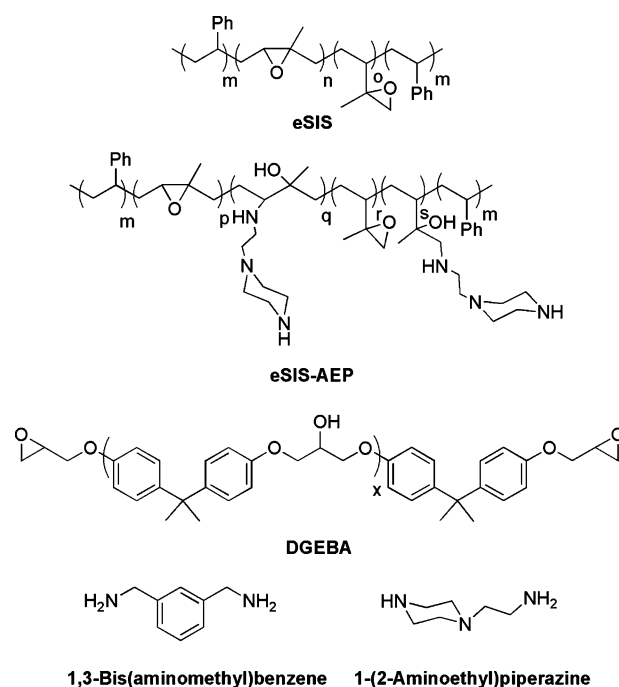


**Figure 1.** Epoxy components and block copolymers used in this study.

**Preparation of eSIS-AEP.** To a solution of eSIS (100 mg, 0.8 mmol epoxy) in anhydrous THF (2.5 mL) was added dropwise a solution of triethylamine (115  $\mu$ L, 0.8 mmol) and excess of 1-(2-aminoethyl)piperazine (0.9 mL, 6.9 mmol) in anhydrous THF (2.5 mL) under a nitrogen atmosphere. The solution was heated to 70 °C for 24 h. Once the reaction was completed, the product was precipitated in petroleum ether, purified by dissolving in THF and precipitating in petroleum ether twice. The pale yellow product was dried under vacuum at 20 °C for 5 h (yield 75%) and stored at –20 °C for characterization.

**Preparation of Nanostructured Thermosets.** Films with a block copolymer content of 23 wt % were prepared as follows: eSIS (100 mg, 0.88 mmol epoxy) or eSIS-AEP (100 mg, 0.66 mmol epoxy, 0.21 mmol –NH) was dissolved in toluene (5 mL) and sonicated for 30 min. DGEBA (213 mg, 1.13 mmol epoxy) was added to the

solution and sonicated for further 30 min. Ancamine (126.1 mg, 1.49 mmol  $-NH$ ) was then added to the resulting solution.

After sonication for 5 min, the solutions were drop-cast on a silicon substrate, previously cleaned with acetone and ethanol, and finally dried with high-purity nitrogen. The solvent was evaporated at room temperature for 12 h (*prior to cure*), and then the films were cured at 80 °C for 180 min (*post cure*) under vacuum. The obtained films had a thickness of  $7 \pm 1 \mu\text{m}$  as determined by a digital micrometer. The reaction extent of each BCP/epoxy system blend prior to cure was calculated to be  $\sim 2\%$  by isothermic differential scanning calorimetry experiments following a previously described procedure.<sup>31</sup>

For the case of DGEBA/hardener, DGEBA/eSIS-AEP and eSIS/hardener blends were prepared to provide a stoichiometric balance between amine protons and epoxy groups.

**Nuclear Magnetic Resonance (NMR).**  $^1\text{H}$  and  $^{13}\text{C}$  NMR spectra were recorded on a Bruker AC-200 spectrometer operating at 200 and 50 MHz, respectively. All spectra were performed using  $\text{CDCl}_3$  as solvent. All areas used in the  $^1\text{H}$  NMR analysis were normalized to the phenyl protons of PS, which were chosen as reference peaks.

**Fourier Transform Infrared Spectroscopy (FT-IR).** The FT-IR spectra of eSIS and eSIS-AEP were measured with a Nicolet 510 P equipment using the KBr disk method. Dry samples were dissolved in  $\text{CH}_2\text{Cl}_2$  (Sigma-Aldrich) and then drop-casted on KBr disks. The spectra were recorded by the average of 32 scans in the standard wavenumber range of  $4000\text{--}400 \text{ cm}^{-1}$ . The baseline was normalized to the  $1458 \text{ cm}^{-1}$  height poly(styrene) (PS) peak.

**Size Exclusion Chromatography (SEC).** Molecular weight distributions and polydispersity indices of the polymers were determined using SEC. Samples were prepared at concentrations near  $5 \text{ mg mL}^{-1}$  in THF. The instrument operates at 30 °C with a Styragel column (HR-4) from Waters covering the molecular weight range of  $5000\text{--}600\,000 \text{ g mol}^{-1}$  at a flow rate of  $1.0 \text{ mL/min}$ . Number- and weight-average molecular weights were calculated by a universal calibration method using PS standards.

**Differential Scanning Calorimetry (DSC).** Calorimetric measurements were made on a TA Q20 differential scanning calorimeter under a dry nitrogen atmosphere. Indium standard was used for calibration. Samples of 5–10 mg were placed in the DSC pan. Dynamic experiments to evaluate the reactivity of eSIS-AEP and eSIS with the epoxy precursors were performed from 20 to 150 °C at a heating rate of  $5 \text{ °C min}^{-1}$ . For dynamic experiments to measure the  $T_g$  values of eSIS and eSIS-AEP samples were equilibrated at 20 °C, heated to 150 °C at  $20 \text{ °C min}^{-1}$ , and held at that temperature for 10 min to remove the thermal history. Then, samples were cooled to  $-80 \text{ °C}$  at a rate of  $20 \text{ °C min}^{-1}$ , held for 10 min, and again heated to 150 °C at  $20 \text{ °C min}^{-1}$ . For dynamic experiments to measure the  $T_g$  values of nanostructured thermosets the samples used were the same than those prepared for AFM measurement. Films were detached from the silicon wafer prior to the DSC scans. Samples were first heated to 150 °C and held at that temperature for 10 min to remove the thermal history. Then, samples were cooled to  $-80 \text{ °C}$  at a rate of  $20 \text{ °C min}^{-1}$ , held for 10 min, and again heated to 150 °C at  $20 \text{ °C min}^{-1}$ . All  $T_g$  values were taken as the midpoint of the transition in the second heating scan.

**Atomic Force Microscopy (AFM).** The morphology features of the nanostructured epoxy thermosetting films were investigated by AFM. AFM images were obtained operating in the soft tapping mode with a scanning probe microscope (Nanoscope IIIa, Multimode from Digital Instruments).

## RESULTS AND DISCUSSION

**Preparation of eSIS-AEP.** The selection of the amine reactive moiety was based on the following analysis: In order to obtain a block copolymer capable of reacting toward DGEBA simultaneously during the curing process of the epoxy system, the incorporated amino reactive moiety should be able to react with DGEBA at a similar temperature than that for DGEBA-hardener reaction (80 °C). To achieve this goal, each of the two amines of the hardener (1,3-bis(aminomethyl)benzene and

1-(2-aminoethyl)piperazine) were evaluated separately. Dynamic DSC experiments were carried out with stoichiometric blends of DGEBA and each amine in order to establish the optimum reaction temperature of each system, taken as the maximum of the exothermic reaction peak. The DGEBA/1,3-bis(aminomethyl)benzene system showed an exothermic peak with  $T_{\text{max}}$  at 89 °C, while the DGEBA/1-(2-aminoethyl)piperazine system had an exothermic peak with  $T_{\text{max}}$  at 74 °C (Supporting Information). From these results 1-(2-aminoethyl)piperazine was expected to be more reactive toward DGEBA than 1,3-bis(aminomethyl)benzene at the epoxy system curing temperature and therefore was chosen to be incorporated to eSIS.

Regarding the modification degree of ePI oxirane rings with AEP, the following considerations were taken. First, a high epoxidation degree is needed to give ePI block miscibility with the epoxy system.<sup>32</sup> Moreover, a high modification degree with AEP would reduce the solubility of the resulting block copolymer in toluene (solvent used in the material preparation). Thus, it was anticipated that a low oxirane ring-opening degree would be enough to give a block copolymer with increased reactivity toward DGEBA retaining the solubility in toluene and the miscibility with the epoxy system.

For the preparation of eSIS-AEP, epoxidized SIS (eSIS) with 100% of epoxidation degree was obtained from SIS following a previously reported epoxidation procedure.<sup>32</sup> In the following step,  $-NH$  side groups were introduced to the epoxidized polyisoprene block (ePI) by partial aminolysis of the oxirane ring of ePI using AEP as the nucleophile to give the corresponding  $\beta$ -amino alcohols. Although AEP might react preferably with the primary amine end rather than the secondary amine end<sup>34</sup> (more sterically hindered), it cannot be excluded that some secondary amine ends react, too. Therefore, Figure 2 shows a simplified chemical structure of eSIS-AEP. This reaction was performed using triethylamine (TEA) as promoter.<sup>35</sup>

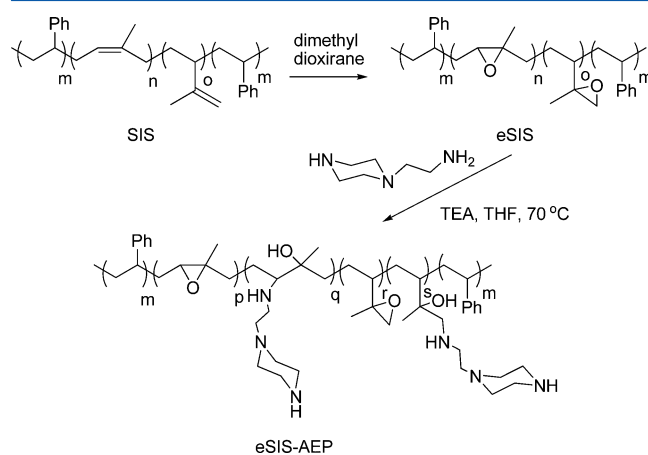


**Figure 2.** Preparation of eSIS-AEP from SIS block copolymer.

Figure 3 displays the  $^1\text{H}$  NMR spectrum of SIS. Signals at 5.1 and 4.8–4.7 ppm are assigned to the olefinic protons  $H_a$  and  $H_b$ , respectively. Such signals completely disappeared after the epoxidation reaction, indicating a quantitative epoxidation of olefins (epoxidation degree of 100% for eSIS). In turn, new signals at 2.7 and 2.6 ppm were formed corresponding to protons  $H_c$  and  $H_d$  of the resulting oxirane rings of eSIS (Figure 4). An epoxidation degree of 100% was obtained for eSIS by

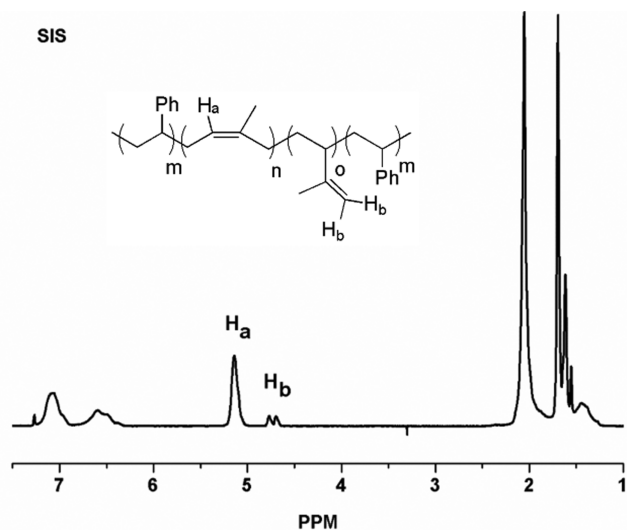


Figure 3.  $^1\text{H}$  NMR spectrum of SIS.

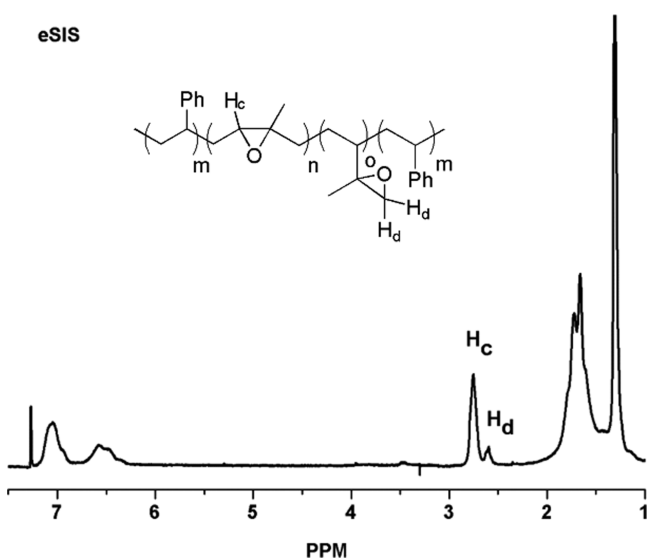


Figure 4.  $^1\text{H}$  NMR spectrum of eSIS.

integration and comparison between normalized areas of oxirane ring protons of eSIS and olefinic protons of SIS. In the  $^1\text{H}$  NMR spectrum of eSIS-AEP (Figure 5) new broad signals between 3.2 and 3.8 ppm correspond to protons  $\text{H}_e$ ,  $\text{H}_f$ ,  $-\text{NH}$ , and  $-\text{OH}$  resulting from the oxirane ring-opening reaction with AEP. As the reaction proceeded, the relative area of oxirane ring protons of eSIS-AEP decreased respect to the same signals of eSIS. From this comparative analysis, an oxirane ring-opening degree of 14% was calculated for eSIS-AEP. It should be noted that new signals of methylene protons that were incorporated by the oxirane ring-opening reaction appeared below 2.4 ppm,<sup>36</sup> which was not a clean region of the spectrum and therefore were not considered to calculate the conversion degree. Although higher oxirane ring-opening degrees were obtained by this strategy (up to 45%), the solubility of the resulting products in organic solvents such as toluene or THF decreased due to the increased hydrogen-bonding interactions between polymeric chains. Therefore, such products were not further considered as modifiers of the epoxy system.

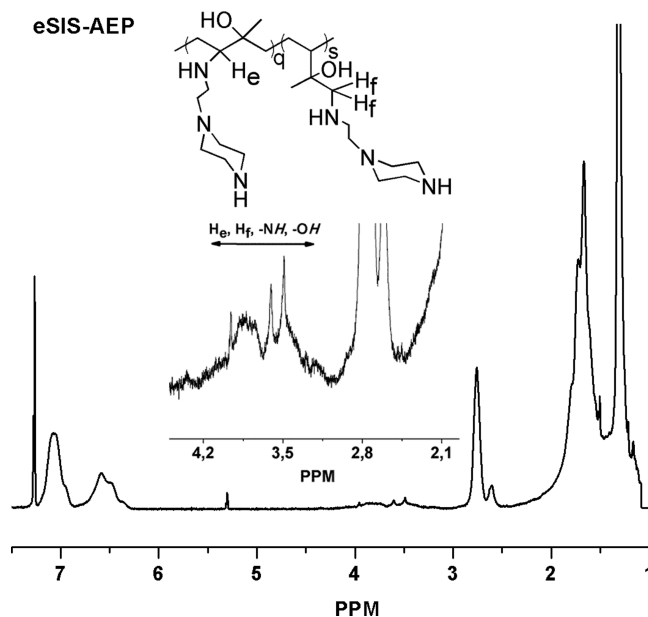


Figure 5.  $^1\text{H}$  NMR spectrum of eSIS-AEP.

In the  $^{13}\text{C}$  NMR spectrum of eSIS (Figure 6) signals at 64.6, 60.5, 35.7, 24.6, and 22.0 ppm were assigned to the epoxidized

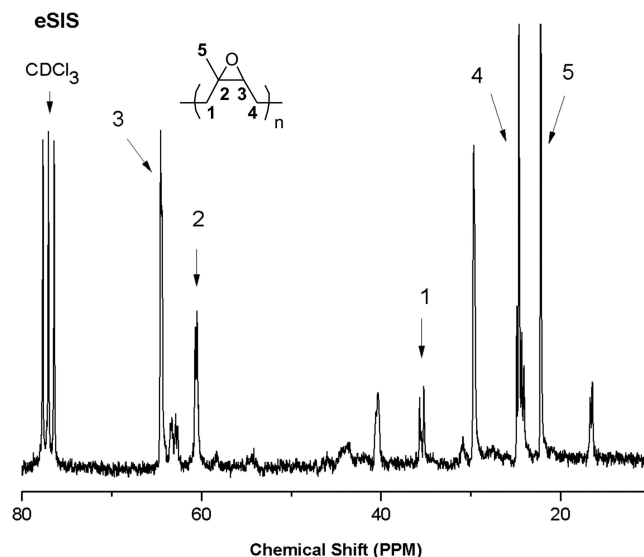


Figure 6.  $^{13}\text{C}$  NMR spectrum of eSIS.

repeating unit carbons 3, 2, 1, 4, and 5, respectively. In the  $^{13}\text{C}$  NMR spectrum of eSIS-AEP (Figure 7) characteristic signals at 53.4 and 41.3 ppm were assigned to the new repeating unit carbons 7, 8, 11 and 6, 9, 10, respectively, confirming the reaction outcome. These signals were of low intensity since the conversion degree was only 14%, as determined by  $^1\text{H}$  NMR spectroscopy. Moreover, the new signals at 27.5 and 34.0 ppm correspond to methylene carbons 4' and 1', respectively. It should be noticed that carbons 2' and 3' could not be assigned because their chemical shift is in a region of the spectrum (60–80 ppm) where the used solvent and the polymer have other signals.

FT-IR spectra of eSIS and eSIS-AEP were measured to further confirm the reaction outcome (Figure 8). A characteristic broad band between 3250 and 3650  $\text{cm}^{-1}$  was observed in



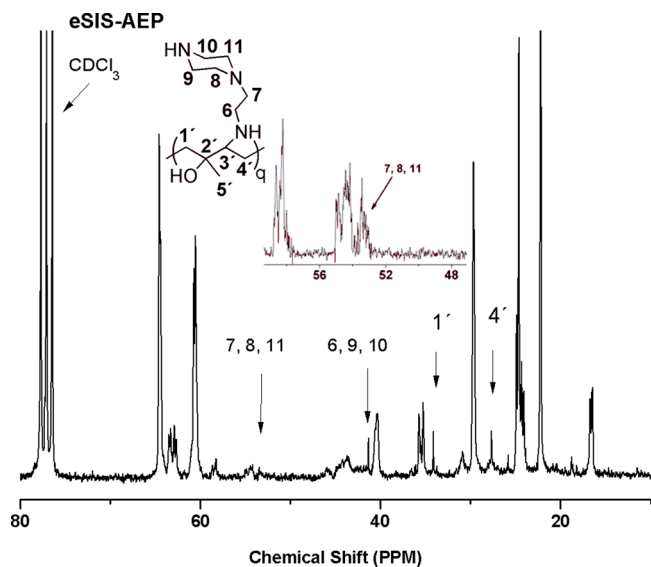


Figure 7.  $^{13}\text{C}$  NMR spectrum of eSIS-AEP.

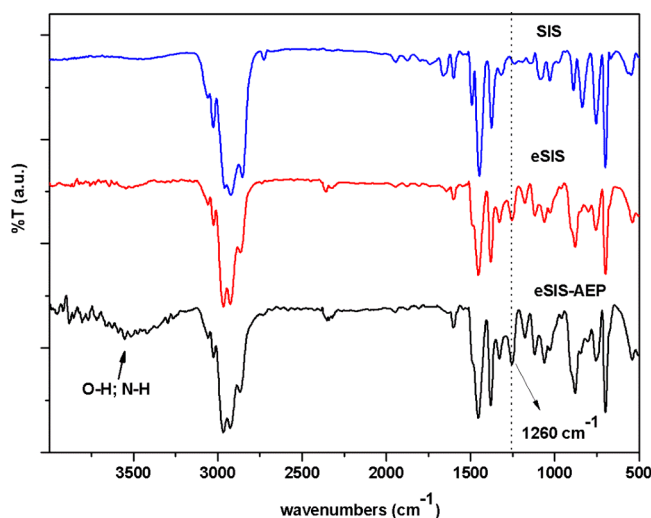


Figure 8. FT-IR spectra of eSIS and eSIS-AEP.

eSIS-AEP spectrum, which is attributed to O–H and N–H stretching vibrations. It was expected that as the ring-opening reaction proceeded, the characteristic epoxy group signal at  $1260\text{ cm}^{-1}$  decreased. As indicated with the arrow in Figure 8, the opposite trend was observed for eSIS-AEP, since the epoxy signal at  $1260\text{ cm}^{-1}$  superposes with the  $\nu(\text{C}-\text{N})$  band at the same frequency,<sup>36</sup> resulting in a band with higher intensity than expected.

The size exclusion chromatography traces of SIS, eSIS, and eSIS-AEP are given in Figure 9. All chromatograms show a major signal corresponding to the triblock copolymer and a minor peak attributed to the presence of lower molecular weight diblock copolymer. A decrease in the elution times from eSIS to eSIS-AEP was observed, which is consistent with an increased molecular weight after oxirane ring-opening reaction. Moreover, SEC traces indicate that the molecular weight distribution of eSIS-AEP was mostly retained compared to eSIS, which confirms that after the ring-opening reaction the block copolymer chain structure was preserved. The absence of a higher molecular weight distribution indicated that no interchain oxirane/amine condensation reaction occurred.

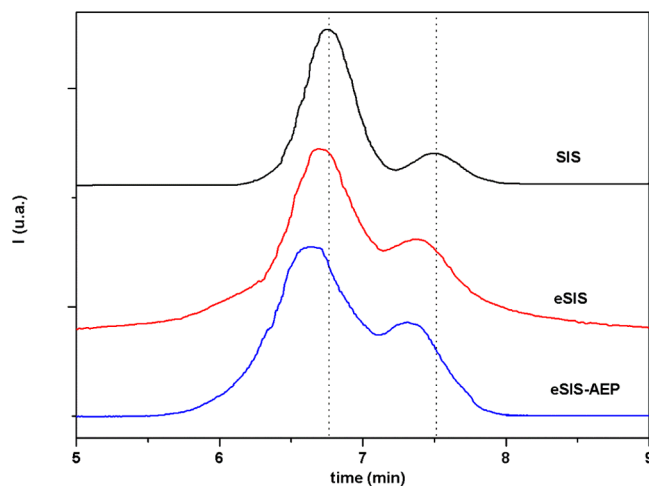


Figure 9. SEC chromatograms for SIS, eSIS, and eSIS-AEP.

Such situation was observed when the reaction was performed at higher temperature ( $80\text{ }^\circ\text{C}$ ) for 24 h (data not shown).

**Reactivity.** According to our previous paper,<sup>31</sup> oxirane rings of DGEBA reacted faster than oxirane rings of eSIS with the hardener, which was attributed to the higher reactivity of primary epoxides against tertiary epoxides toward nucleophilic attack. Since the synthesized eSIS-AEP contains –NH side groups, it is expected that its reactivity against the epoxy precursors increases. In fact, the obtained block copolymer should be reactive toward the primary oxirane rings of DGEBA. In order to prove the ability of eSIS-AEP to react toward DGEBA, dynamic DSC experiments were performed from 20 to  $150\text{ }^\circ\text{C}$  as shown in Figure 10. Gratifyingly, eSIS-AEP/

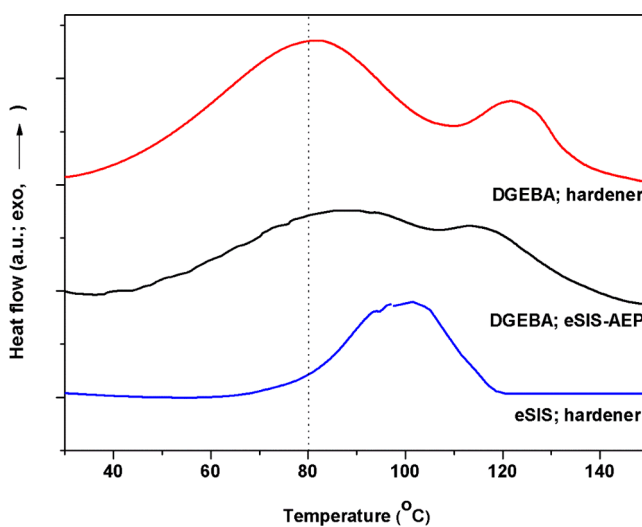
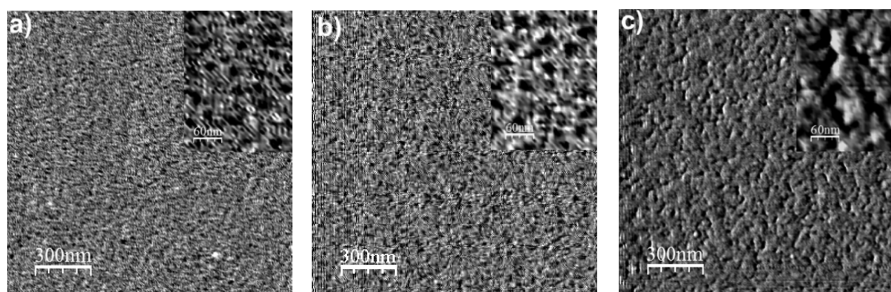


Figure 10. Dynamic DSC from 20 to  $150\text{ }^\circ\text{C}$  for DGEBA-hardener, eSIS-AEP/DGEBA, and eSIS/hardener.

DGEBA showed an exotherm with  $T_{\text{max}}$  at  $87\text{ }^\circ\text{C}$ , which corresponds to the epoxy/amine condensation and is very close in temperature to the  $T_{\text{max}}$  ( $81\text{ }^\circ\text{C}$ ) of DGEBA/hardener exotherm. Therefore, it is expected that at the epoxy system curing temperature ( $80\text{ }^\circ\text{C}$ ) ePI-AEP subchains can participate in the epoxy/amine condensation reaction. Moreover, it is worth noting from Figure 10 that the  $T_{\text{max}}$  of eSIS-AEP/DGEBA ( $87\text{ }^\circ\text{C}$ ) is considerably lower than that for eSIS/hardener ( $100\text{ }^\circ\text{C}$ ), indicating that eSIS-AEP is more reactive



**Figure 11.** Tapping mode AFM phase image of block copolymer (23 wt %)/DGEBA + hardener blends for (a) eSIS-AEP before curing, (b) eSIS-AEP after curing, and (c) eSIS after curing.

than eSIS toward the epoxy precursors at the curing temperature. From DSC experiments  $\Delta H$  of the exothermic process was determined to be  $98 \pm 2 \text{ kJ mol}^{-1}$ , which is consistent with previously reported epoxy/amine condensation enthalpy values.<sup>37</sup> Even though the homopolymerization/etherification of DGEBA could be initiated by tertiary amines of AEP without significant changes in the total enthalpy value,<sup>37–39</sup> this process would occur at higher temperatures than the curing temperature.<sup>40</sup> Therefore, in the current system the main occurring reaction is the epoxy/amine condensation.

It is worth noting that a second exothermic process at  $120 \text{ }^\circ\text{C}$  was observed in formulations with DGEBA, likely due to the homopolymerization of DGEBA molecules that did not react at lower temperatures with the hardener (epoxy/amine condensation) due to the high heating rate of the dynamic DSC experiment. This reaction could have been initiated by tertiary amines of AEP. However, this process occurs well above the curing temperature ( $80 \text{ }^\circ\text{C}$ ) and therefore does not take place in the epoxy curing conditions of the present work.

Transparent films were obtained by blending eSIS-AEP (23 wt %) with the epoxy system, giving evidence that no macrophase separation occurred due to the miscibility of ePI-AEP block with the epoxy system.

With regards to the miscibility and phase behavior of PS block and the epoxy precursors, previous works by Meng et al.<sup>14</sup> and Hoppe et al.<sup>41</sup> indicated that blends of DGEBA and PS chains with a similar molecular weight than that for PS blocks of eSIS-AEP (19 000 g/mol) are miscible at  $80 \text{ }^\circ\text{C}$  for a PS composition of 6%. However, the presence of the hardener molecules (1-(2-aminoethyl)piperazine and 1,3-bis-(aminomethyl)benzene) could have the opposite effect on the miscibility of the system, making the PS blocks immiscible in the epoxy precursors at the curing temperature. In order to evaluate this effect, blends consisting on DGEBA/hardener and polystyrene with the identical molecular weight (19 000 g/mol) than PS blocks of eSIS-AEP have been prepared. It was found that before curing DGEBA/hardener/PS blends were cloudy at room temperature, indicating a macrophase separation behavior. By heating the material at  $80 \text{ }^\circ\text{C}$  (curing temperature), blends remained opaque, suggesting that PS blocks of eSIS-AEP are immiscible with the epoxy precursors at the curing temperature.

Therefore, by combining an epoxy miscible block (ePI-AEP) and an epoxy immiscible block (PS), a self-assembly mechanism was likely to be operative in eSIS-AEP/DGEBA/hardener systems. Moreover, we anticipated that the ability of eSIS-AEP to react toward DGEBA during the curing process would have morphological consequences in the obtained material, and therefore it was analyzed by AFM.

**Morphology of Nanostructured Materials with eSIS-AEP.** A representative AFM phase image of eSIS-AEP/epoxy system in the uncured state (*prior to cure*) is presented in Figure 11a. The block copolymer self-assembles into well-dispersed spherical nanodomains as clearly observed in the micrograph. After curing (*post cure*), the material preserves the spherulike morphology as shown in Figure 11b. While we do not know the exact structure on the material in the region surrounding the spherulike nanodomains in the cross-linked product, two limiting situations can be advanced. In one limit, cross-linking might expel the ePI-AEP blocks leading to a core-shell structure with nearly pure ePI-AEP surrounding the PS cores. Formation of discrete domains of ePI-AEP should be evidenced by a glass transition in a calorimetry experiment. In the second possible scenario, the ePI-AEP subchains remain mixed and linked with the epoxy matrix, leading to plasticization and/or network damage. For a comparative analysis Figure 11c shows AFM phase image of eSIS/epoxy system after curing, which represents an example of the first limiting situation where the ePI block is partially expelled during curing on the basis of reaction induced microphase separation mechanism.<sup>31</sup> As it is clearly seen, the obtained morphology consists of distorted spherulike nanostructures with some interconnections between domains, which appear to be composed of aggregates of the primarily obtained spherical morphologies, as shown in the inset of Figure 11c. Therefore, the initially obtained spherulike nanodomains in eSIS/epoxy system<sup>31</sup> before curing were strongly affected by the gradual ePI subchains demixing process as the curing reaction progressed. On the contrary, the initial spherulike morphology displayed by eSIS-AEP/epoxy system was mainly preserved after curing, which strongly suggest that reaction induced microphase separation process of the interpenetrated ePI-AEP subchains was avoided.

Figure 12 displays DSC traces obtained from eSIS and eSIS-AEP. It was observed that eSIS showed a first  $T_g$  at  $25 \text{ }^\circ\text{C}$  corresponding to epoxidized poly(isoprene) block. For the case of eSIS-AEP the first glass transition temperature decreased in  $12 \text{ }^\circ\text{C}$  with respect to that of eSIS likely due to the increase of free volume by the incorporation of pendant groups in combination with the loss of 14% of rigid oxirane rings. A second  $T_g$  was observed for eSIS and eSIS-AEP at around  $87 \text{ }^\circ\text{C}$ , which corresponds to the poly(styrene) blocks. However, this  $T_g$  was barely discernible due to the used scale in Figure 12.

Important differences were accounted for in the phase behavior of nanostructured cured materials, as presented in Figure 12. First, the eSIS/DGEBA-hardener (ER) system showed an ePI-rich phase with a  $T_g$  at  $27 \text{ }^\circ\text{C}$ , confirming that partial ePI demixing process occurred during curing. Interestingly, such a situation was not evidenced for eSIS-AEP/ER

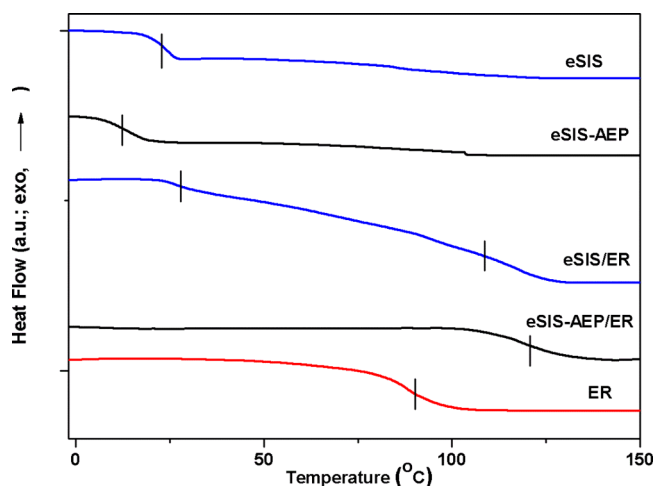


**Figure 12.** DSC curves of the second heating scan for eSIS, eSIS-AEP, and eSIS/ER, and eSIS-AEP/ER cured blends.

system, which indicated that no ePI-AEP-rich phase was formed during curing. This result strongly suggested that the reactivity of ePI-AEP block toward DGEBA during curing prevented phase separation from the cross-linked network. The fact that the ePI-AEP block remained mixed with the matrix affected the epoxy system glass transition temperature which increased in 10 °C for eSIS-AEP/ER with respect to eSIS/ER as a consequence of a reduction of the free volume of the polymeric matrix.

Previous works by Bates and colleagues<sup>25</sup> and Guo and co-workers<sup>17</sup> reported similar shifts to higher temperatures in the range of 16–25 °C between the  $T_g$  of epoxy and epoxy-BCP systems. It is worth noting that in the present work the shift was slightly higher (30 °C), likely due to the presence of AEP in the hardener, which confers flexibility to the epoxy network.

The  $T_g$  corresponding to PS blocks in the BCP/epoxy systems was not visualized in Figure 12 due to the low amount of PS (approximately 7 wt %) in the materials.

These results are in good agreement with the AFM micrographs and support the second limiting situation for the case of eSIS-AEP, where the nanostructured domains consist of polystyrene blocks and the ePI-AEP subchains remain mixed and linked to the cross-linked matrix, as shown in Figure 13. The lack of reactivity of eSIS toward the epoxy resin conducted

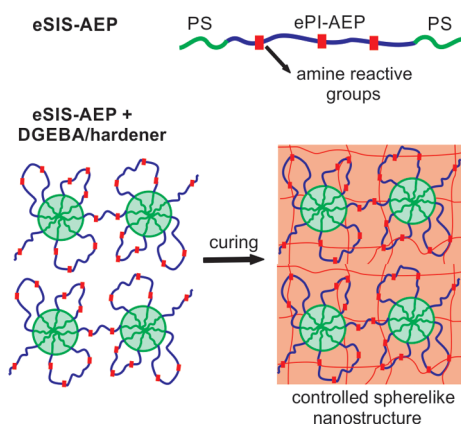


**Figure 13.** Schematic illustration of the formation of spherulike nanodomains in the eSIS-AEP + DGEBA/hardener system.

to a very different scenario where demixed ePI blocks surrounded the PS spherulike cores in an irregular way, affecting not only the nanodomain size but also the morphology.

## CONCLUSION

Oxirane ring-opening reaction of an epoxidized poly(styrene-*b*-isoprene-*b*-styrene) (eSIS) block copolymer was performed using 1-(2-aminoethyl)piperazine as nucleophile to give a novel block copolymer (eSIS-AEP) capable of reacting toward diglycidyl ether of bisphenol A (DGEBA) during the curing reaction of the epoxy system. The incorporation of eSIS-AEP to the epoxy system as a modifier led to nanostructured materials with spherulike nanodomains that were formed before curing by self-assembling of poly(styrene) blocks. Conversely to the typical ePI demixing process encountered for eSIS during the curing stage, for the case of eSIS-AEP the nanodomain morphology was preserved, which indicated that no ePI-AEP demixing process occurred as a consequence of the enhanced reactivity of eSIS-AEP with DGEBA. These results demonstrate that the obtained nanostructure in an epoxy thermoset can be modulated by incorporating a block copolymer containing an epoxy miscible block with enhanced reactivity toward the epoxy system.

## ASSOCIATED CONTENT

### Supporting Information

Dynamic DSC experiments for DGEBA/1,3-bis(aminomethyl)-benzene and DGEBA/1-(2-aminoethyl)piperazine systems. This material is available free of charge via the Internet at <http://pubs.acs.org>.

## AUTHOR INFORMATION

### Corresponding Authors

\*E-mail [goyanes@df.uba.ar](mailto:goyanes@df.uba.ar) (S.G.).

\*E-mail [norma@qo.fcen.uba.ar](mailto:norma@qo.fcen.uba.ar) (N.B.D.).

### Notes

The authors declare no competing financial interest.

## ACKNOWLEDGMENTS

The authors thank the financial support of UBACyT (No. 20020100100350 and 200220100100142), ANPCyT (PICT-2012-0717 and PICT-2012-1093), and CONICET (PIP 2013-2015, 11220120100508CO and 11220110100370CO) and the fellowship of H.G. from Argentina. The authors are also thankful for funding from the European Community (POCO project, 7th FP, NMP-213939).

## REFERENCES

- (1) Wu, S.; Guo, Q.; Peng, S.; Hameed, N.; Kraska, M.; Stühn, B.; Mai, Y.-W. *Macromolecules* **2012**, *45*, 3829–3840.
- (2) Rebizant, V.; Venet, A.-S.; Tournilhac, F.; Girard-Reydet, E.; Navarro, C.; Pascault, J.-P.; Leibler, L. *Macromolecules* **2004**, *37*, 8017–8027.
- (3) Dean, J. M.; Verghese, N. E.; Pham, H. Q.; Bates, F. S. *Macromolecules* **2003**, *36*, 9267–9270.
- (4) Declet-Perez, C.; Redline, E. M.; Francis, L. F.; Bates, F. S. *ACS Macro Lett.* **2012**, *1*, 338.
- (5) Hillmyer, M. A.; Lipic, P. M.; Hajduk, D. A.; Almdal, K.; Bates, F. S. *J. Am. Chem. Soc.* **1997**, *119*, 2749.
- (6) Lipic, P. M.; Bates, F. S.; Hillmyer, M. A. *J. Am. Chem. Soc.* **1998**, *120*, 8963.

- (7) Maiez-Tribut, S.; Pascault, J. P.; Soulé, E. R.; Borrajo, J.; Williams, R. J. J. *Macromolecules* **2007**, *40*, 1268–1273.
- (8) Xu, Z.; Zheng, S. *Polymer* **2007**, *48*, 6134–6144.
- (9) Ritzenthaler, S.; Court, F.; David, L.; Girard-Reydet, E.; Leibler, L.; Pascault, J.-P. *Macromolecules* **2002**, *35*, 6245–6254.
- (10) Ritzenthaler, S.; Court, F.; Girard-Reydet, E.; Leibler, L.; Pascault, J. P. *Macromolecules* **2003**, *36*, 118–126.
- (11) Yu, R.; Zheng, S. *Macromolecules* **2011**, *44*, 8545–8557.
- (12) Ruiz-Pérez, L.; Royston, G. J.; Fairclough, J. P. A.; Ryan, A. J. *Polymer* **2008**, *49*, 4475.
- (13) Meng, F.; Zheng, S.; Zhang, W.; Li, H.; Liang, Q. *Macromolecules* **2006**, *39*, 711–719.
- (14) Meng, F.; Zheng, S.; Li, H.; Linag, Q.; Liu, T. *Macromolecules* **2006**, *39*, 5072–5080.
- (15) Meng, F.; Xu, Z.; Zheng, S. *Macromolecules* **2008**, *41*, 1411–1420.
- (16) Ocando, C.; Fernández, R.; Tercjak, A.; Mondragon, I.; Eceiza, A. *Macromolecules* **2013**, *46*, 3444.
- (17) Hameed, N.; Guo, Q.; Xu, Z.; Hanley, T. L.; Mai, Y.-W. *Soft Matter* **2010**, *6*, 6119.
- (18) Romeo, H. E.; Zucchi, I. A.; Rico, M.; Hoppe, C. E.; Williams, R. J. J. *Macromolecules* **2013**, *46*, 4854–4861.
- (19) Zheng, S. Nanostructured Epoxies by the Use of Block Copolymers. In *Epoxy Polymer: New Materials and Innovations*; Pascault, J. P., Williams, R. J. J., Eds.; Wiley-VCH: Weinheim, Germany, 2010.
- (20) Wu, J. X.; Thio, Y. S.; Bates, F. S. *J. Polym. Sci., Part B: Polym. Phys.* **2005**, *43*, 1950–1965.
- (21) Dean, J. M.; Grubbs, R. B.; Saad, W.; Cook, R. F.; Bates, F. S. *J. Polym. Sci., Part B: Polym. Phys.* **2003**, *41*, 2444–2456.
- (22) Thio, Y. S.; Wu, J. X.; Bates, F. S. *J. Polym. Sci., Part B: Polym. Phys.* **2009**, *47*, 1125–1129.
- (23) Liu, J.; Sue, H. J.; Thompson, Z. J.; Bates, F. S.; Dettloff, M.; Jacob, G.; Verghese, N.; Pham, H. *Macromolecules* **2008**, *41*, 7616–7624.
- (24) Gerard, P.; Boupat, N. P.; Fine, T.; Gervat, L.; Pascault, J. P. *Macromol. Symp.* **2007**, *256*, 55–64.
- (25) Thio, Y. S.; Wu, T. J.; Bates, F. S. *Macromolecules* **2006**, *39*, 7187–7189.
- (26) Liu, J. D.; Thompson, Z. J.; Sue, H.-S.; Bates, F. S.; Hillmyer, M. A.; Dettloff, M.; Jacob, G.; Verghese, N.; Pham, H. *Macromolecules* **2010**, *43*, 7238–7243.
- (27) Dean, J. M.; Lipic, P. M.; Grubbs, R. B.; Cook, R. F.; Bates, F. S. *J. Polym. Sci., Part B: Polym. Phys.* **2001**, *39*, 2996–3010.
- (28) He, X.; Liu, Y.; Zhang, R.; Wu, Q.; Chen, T.; Sun, P. *J. Phys. Chem. C* **2014**, *118*, 13285–13299.
- (29) Grubbs, R. B.; Dean, J. M.; Broz, M. E.; Bates, F. S. *Macromolecules* **2000**, *33*, 9522–9534.
- (30) Rebizant, V.; Abetz, F.; Tournilhac, F.; Court, F.; Leibler, L. *Macromolecules* **2003**, *36*, 9889–9896.
- (31) Garate, H.; Mondragon, I.; D'Accorso, N. B.; Goyanes, S. *Macromolecules* **2013**, *46*, 2182–2187.
- (32) Garate, H.; Mondragon, I.; Goyanes, S.; D'Accorso, N. *J. Polym. Sci., Part A: Polym. Chem.* **2011**, *49*, 4505–4513.
- (33) Bonnaud, L.; Pascault, J. P.; Sautereau, H.; Zhao, J. Q.; Jia, D. M. *Eur. Polym. J.* **2004**, *40*, 2637–2643.
- (34) Rosenberg, B. A. *Makromol. Chem., Macromol. Symp.* **1987**, *7*, 17–26.
- (35) Wu, J.; Xia, H.-G. *Green Chem.* **2005**, *7*, 708–710.
- (36) Zhu, L.; Tu, C.; Zhu, B.; Su, Y.; Pang, Y.; Yan, D.; Wu, J.; Zhu, X. *Polym. Chem.* **2011**, *2*, 1761–1768.
- (37) Ooi, S. K.; Cook, W. D.; Simon, G. P.; Such, C. H. *Polymer* **2000**, *41*, 3639–3649.
- (38) Klute, C. H.; Viehmann, W. *J. Appl. Polym. Sci.* **1961**, *12*, 86–95.
- (39) Rozenberg, B. A. *Adv. Polym. Sci.* **1986**, *75*, 113–165.
- (40) Foix, D.; Jiménez-Piqué, E.; Ramis, X.; Serra, A. *Polymer* **2011**, *52*, 5009–5017.
- (41) Meng, F.; Zheng, S.; Li, H.; Liang, Q.; Liu, T. *Macromolecules* **2006**, *39*, 5072–5080.
- (42) Hoppe, C. E.; Galante, M. J.; Oyanguren, P. A.; Williams, R. J. J. *Polym. Eng. Sci.* **2002**, *42*, 2361–2368.